Proceedings of the 11th ICPMG 2026
11th International Conference on Physical Modelling in Geotechnics
8-12 June 2026, Zurich, Switzerland

Centrifugal model test on the stability of bucket foundation revetment under different backfill materials

Y.F. Guan

Nanjing Hydraulic Research Institute, Nanjing, China, yfguan@nhri.cn

X. Han, Z.J. Pan

Nanjing Hydraulic Research Institute, Nanjing, China, xhan@nhri.cn, 210204010009@hhu.edu.cn

ABSTRACT: The bucket foundation structure is a lightweight, thin-walled, multi-compartment structure suitable for muddy sea areas. When used as a revetment, this structure primarily is subjicted to backfill loads and involves complex bucket-soil interaction. This study investigates the stability of bucket foundation revetments under different backfill materials through geotechnical centrifuge model tests. The results indicate that the bucket foundation revetment satisfies the stability requirements under all test conditions. During backfilling inside the bucket, the main structural displacement was settlement, with resistance at the bottom of the bucket and friction on the inner wall being the dominant resistive forces. During backfilling on the landside, the structural displacement was significantly influenced by the vertical load sharing ratio between the bucket and the soil. When backfilled with soft clay, the structure predominantly experienced sliding towards the seaside, with the soil on the seaside of the lower bucket providing substantial resistance. When backfilled with standard sand and block stone, the bucket mainly tilted towards the landside, with the soil near the landside at the bottom and within the compartments offering greater resistance. The results of this study will provide a reference for the design and construction of backfilling for bucket foundation revetments.

1 INTRODUCTION

The bucket foundation structure is a thin-walled multi compartment structure suitable for muddy sea areas, typically prefabricated from reinforced concrete. A single bucket is divided into an upper structure and a lower bucket, and it sinks to the seabed through self-weight and negative pressure (Shen et al., 2017), as shown in Figure 1. When used as a breakwater, the bucket foundation primarily bears wave loads and is significantly influenced by changes in water level (Pan et al., 2023). When employed as a revetment, the structure primarily suffers backfill loads, and is more complicated by multiple factors such as bucket size and backfill load situation (Zhang and Gui, 2018) , which merit further research.

A number of studies have been conducted to investigate the behavior of bucket foundation structures through geotechnical centrifugal model tests. Xu et al. (2014) examined the stress characteristics during the penetration process of bucket foundation structures, identifying the critical resistance value associated with bucket settlement. Chen and Li (2016) simulated the effects of wave loads on bucket foundation breakwater structures under hyper-gravity conditions, using both quasi-static and cyclic forces. Their work provided insights into the deformation stability characteristics and potential failure modes of the structure at various stages. Nie et al. (2016) performed geotechnical centrifuge model tests to study the displacement of bucket foundation structure under layered backfilling. Their results showed that insufficient embedding depth in silt can cause the bucket to slide towards the seaside, and they suggested that backfilling with bagged sand and increasing the embedment depth would improve stability. Shen et al. (2019) investigated the displacement patterns of bucket foundations under layered backfill sludge conditions, noting a primary displacement toward the seaside, accompanied by some deflection towards the landside. They proposed corresponding displacement limit criteria for these conditions. Despite these valuable contributions, the interaction mechanism between bucket and soil under backfill load is not yet clear. It is necessary to comprehensively study the stability of bucket under different typical backfill materials through geotechnical centrifuge model tests.

This article conducted geotechnical centrifuge model tests by integrating existing technologies and improving methods to analyze the stability of bucket foundation revetments under different backfill materials. Furthermore, based on the mechanism of bucket-soil interaction, the stability discrimination calculation methods and measures to reduce displacement under the conditions of backfilling inside and behind the bucket were proposed.

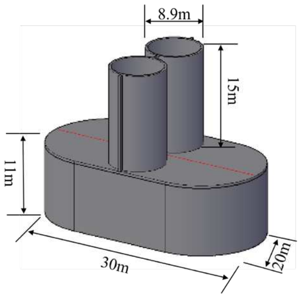

Figure 1. Bucket foundation structure.

2 MATERIALS & METHODOLOGY

2.1 Test plan

Based on a special engineering background and experimental conditions, three sets of centrifugal model tests were conducted to study the influence of fill materials on the force and deformation of bucket foundation structures. The foundation soil layer is composed of soft clay, silty clay and sand from top to bottom. The prototype bucket is embedded to a depth of 1.0 m into the silty clay layer. The elliptical lower bucket has a major axis of 30m and a minor axis of 20 m. To increase the self-weight of the structure and effectively reduce horizontal displacement and overturning, clay was selected to backfill the upper bucket in accordance with the engineering construction conditions. The test conditions are shown in *Table 1*.

The centrifugal model tests were conducted on the bucket foundation revetment under unilateral backfilling using NHRI-50g.t. This device has an effective rotation radius of 2.25 m, a maximum load capacity of 200 kg, a maximum acceleration of 250 g, and multiple channels for strain and voltage signal data acquisition. More detailed specifications of the centrifuge apparatus can be found in our previous work (Guan et al., 2025) . And the model similarity scale was selected as 80. Due to the small size of the model, aluminum alloy was selected as a substitute for reinforced concrete, and the wall thickness of the model was determined based on the theory of equivalent bending stiffness. The simulated foundation soil was sourced from the engineering site and prepared in layers from top to bottom within the model box. Cohesive soil was controlled by undrained shear strength (c_u), while non-cohesive soil was controlled by dry density (γ_d).

2.2 Test layout

The test layout is shown in Figure 2. The monitoring sensors include non-contact laser displacement sensors, soil pressure sensors, and pore pressure sensors. The simulated water depth corresponds to a prototype depth of approximately 5.5 m.

Table 1. Centrifugal model test scheme and main physical and mechanical property indexes of soil layers for unilateral backfilling of bucket foundation revetment.

Model	**Backfilling materials on the landside**	**Backfilling height of prototype on the landside (m)**	**Water content (%)**	**Volumetric weight (kN·m^3)**	**Cohesion intercept (kPa)**	**Friction angle (°)**
M1	Soft clay	12	110~150	14.5~15.5	5~10	0~5
M2	Standard sand	12	/	15.5~16.5	0~3	20~30
M3	Block stone	12	/	19.0~21.0	0	40~50

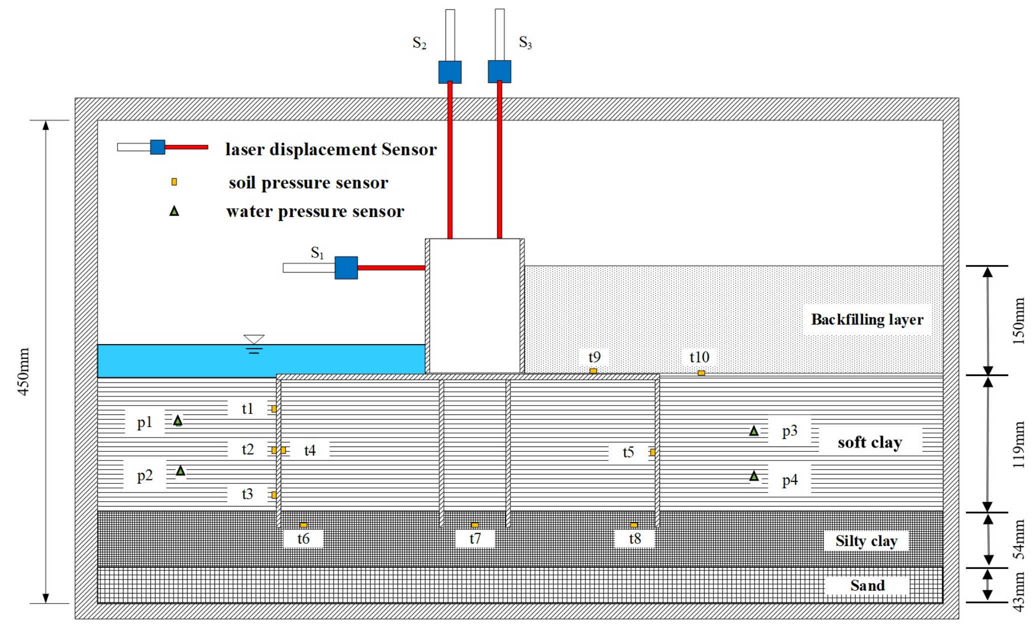

(a) Sectional view

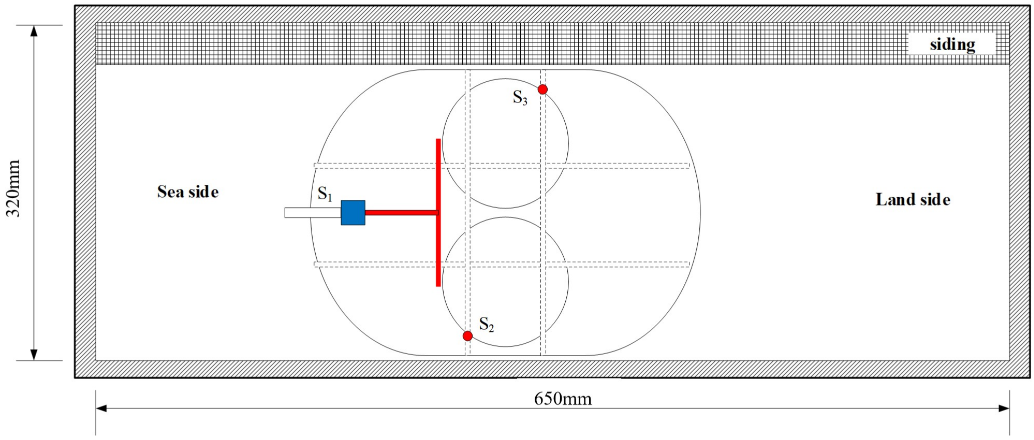

(b) Plan view

Figure 2. Layout of centrifuge model test.

3 RESULTS & DISCUSSION

3.1 Bucket displacement

For ease of analysis, the construction and operation periods of backfilling inside the bucket are denoted as StageI and Stage II, respectively. And the construction and operation periods of backfilling on the landside are denoted as Stage III and Stage IV, respectively. All displacement data presented in this study have been converted to the prototype scale based on the model similarity scale of 80.

Based on the measurement results from S_1, the horizontal displacement curve of the upper part of the bucket was plotted, as shown in Figure 2. The results indicate that no significant horizontal displacement occurred during stages I and II. However, the horizontal displacement patterns in stages III and IV differed due to the influence of different backfill materials: (1) After 245 days, the horizontal displacement of M1 developed towards the seaside, reaching -33 mm by the end of stage III, and continued to increase in stage IV, ultimately reaching approximately -35 mm. (2) After around 233 days, the horizontal displacement of M2 shifted towards the landside, rapidly increasing to 31 mm, and stabilized at approximately 33 mm by the end of stage IV. (3) After about 226 days, the horizontal displacement of M3 also developed towards the landside, rapidly increasing to 41 mm, and stabilized at approximately 43 mm by the end of stage IV. These findings suggest that when backfilling with viscous materials of high water content, larger lateral loads cause the upper part of the bucket to shift towards the seaside. In contrast, when backfilling with heavy sandy materials, larger loads acting on the landside cover plate result in the upper part of the bucket moving towards the landside.

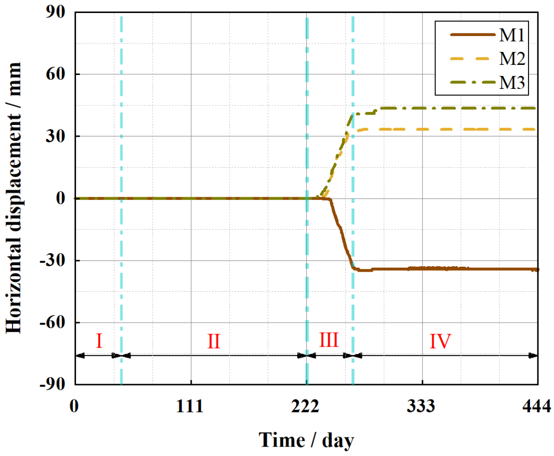

Figure 3. Horizontal displacement variation curve.

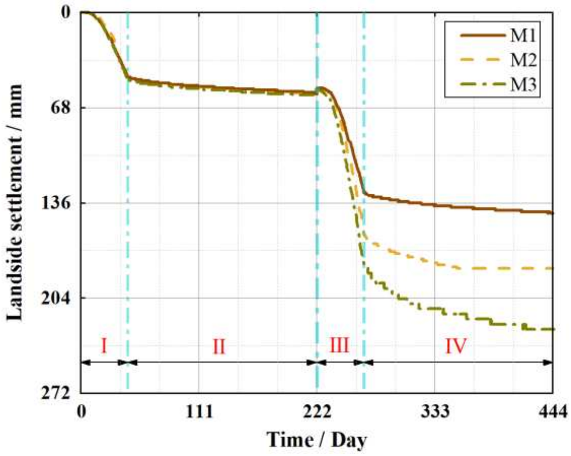

Figure 5. Landside settlement variation curve.

The settlement variations of the measurement points S_2 and S_3 are presented in Figure 4 and Figure 5, respectively. During stages I and II, the settlement trends on both the seaside and landside were similar, with settlements of approximately 47 mm in stage I, increasing to 58 mm in stage II. To minimize errors introduced by backfilling under 1g conditions, the difference in settlement measurements between stages I and II under 1g was used to adjust the initial values for stage III. The results indicated distinct differences in settlement on the seaside and landside during stages III and IV: (1) The settlement variation amplitude at M1 was the smallest, with final settlements of 132 mm on the seaside and 144 mm on the landside. (2) The final settlement on the landside of M2 was approximately 147 mm, while the seaside settlement was about 183 mm. (3) M3 experienced the fastest settlement development, with the maximum settlement on the landside reaching about 226 mm, while the seaside settlement was 177 mm. Additionally, the subsidence rate was higher in stages I and III compared to stages II and IV, likely due to the influence of changes in the supergravity field.

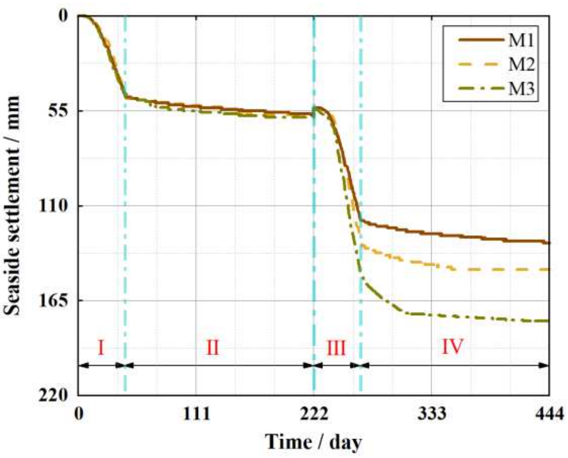

Figure 4. Seaside settlement variation curve.

The structural turning angle was calculated using Eq. (1) based on the settlement changes measured at different stages, and the resulting curve is shown in Figure 6.

$$\theta=\arctan((s_3-s_2) / d) \quad (1)$$

During stages I-II, the rotation angle of the bucket remained close to 0°. In stage III, the bucket began to exhibit a turning angle towards the landside, with the rate of change varying. In stage IV, the increase in the bucket rotation angle was also different due to differences in the magnitude of the load continuously applied to the cover plate. The specific descriptions are as follows: (1) Due to the low weight and high water content of the backfill material in M1, the change in rotation angle was relatively small, reaching approximately 0.06° by the end of stage III and increasing slightly to 0.08° in stage IV. (2) M2 showed a more rapid development towards the landside in stage III, reaching 0.17°, and further increasing to 0.23° in stage IV. (3) In M3, due to the heavier backfill material, the rotation angle of the bucket changed significantly, reaching 0.21° at the end of stage III and 0.32° at the end of stage IV.

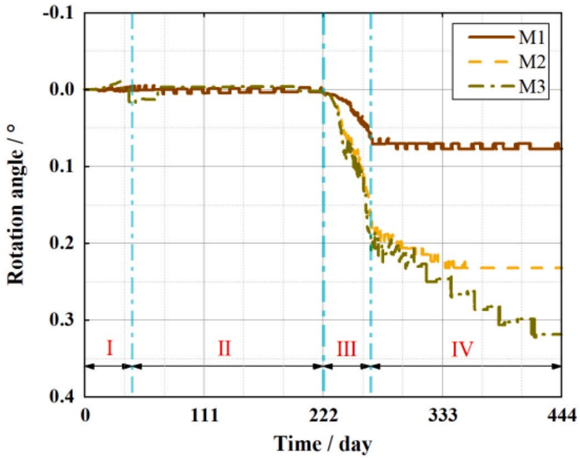

Figure 6. Rotation angle variation curve.

The observed displacement patterns result from the combined effects of lateral and vertical loads induced by different backfill materials. Cohesive backfill generates larger horizontal loads, promoting sliding towards the seaside, while heavier, non-cohesive backfill increases vertical loads and overturning moments, driving rotation towards the landside.

3.2 Soil pressure

Based on the monitoring results, the soil pressure at key locations after the completion of each stage was analysed. Besides, the final measured values were compared with the theoretical values based on Rankine's soil pressure theory. Here, σ_0 is the theoretical value of static soil pressure, σ_a is the theoretical value of active soil pressure, and σ_p is the theoretical value of passive soil pressure.

Figure 7 shows the soil pressure results on the seaside of the lower bucket (t1-t3). The measured values at the end of stage II were close to the static soil pressure, and the measured values at the end of stage IV reflected the passive soil pressure state. The highest measurements were obtained for M1, which was influenced by the bucket sliding towards the seaside. However, the buckets in M2 and M3 overturned towards the landside, with similar final results for both.

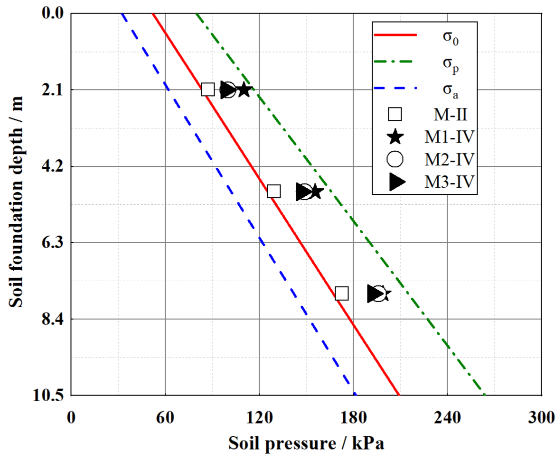

Figure 7. Comparison between measured and theoretical soil pressure values on the seaside of the lower bucket.

Figure 8 shows the final results of the lateral soil pressure at the inner wall of the lower bucket (t4-t5). Due to the displacement of the bucket, the soil in the internal compartment was in a state of passive soil pressure. The soil pressure at t4 was slightly higher than the theoretical value of static soil pressure, while the soil pressure at t5 approached the theoretical value of passive soil pressure as the backfill load increased.

It should be noted that the soil pressure state is governed by both soil depth and the compression condition. Although t4 is located on the opposite side of the wall, it is at a similar depth to t2 and therefore exhibits comparable stress levels. The passive earth pressure observed at t1–t3 is mainly caused by the horizontal movement of the bucket towards the seaside, which compresses the surrounding soil and mobilizes passive resistance. In contrast, the passive state at t4 is induced by the vertical settlement of the bucket, which leads to compression of the soil within the compartment and generates additional pressure on the inner wall of the lower bucket.

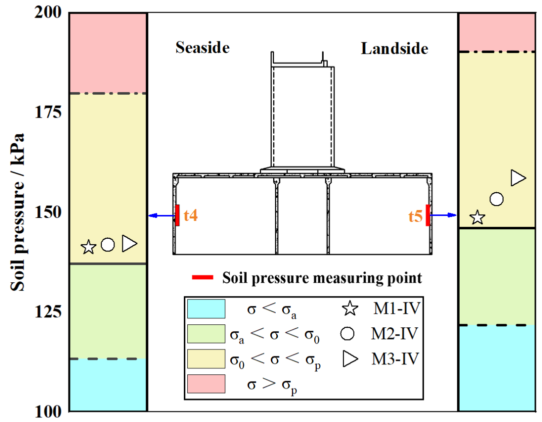

Figure 8. Comparison between measured and theoretical values of soil pressure at the inner wall of the lower bucket.

The schematic diagrams of the soil pressure distribution at the bottom of the bucket (t6-t8) at the end of stages II and IV are shown in Figure 9 and Figure 10. During the backfilling stage inside the bucket, the distribution of soil pressure at the bottom was influenced by the extent of the backfill load, resulting in a distribution that approximated a parabolic shape, with the pressure at the center being slightly higher than at the sides. During the landside backfilling stage, the distribution of soil pressure at the bottom of the bucket gradually evolved into a trapezoidal shape, with the highest pressure on the landside and the lowest pressure on the seaside. Moreover, as the backfill load increased, the difference in soil pressure between the seaside and the landside also became more pronounced.

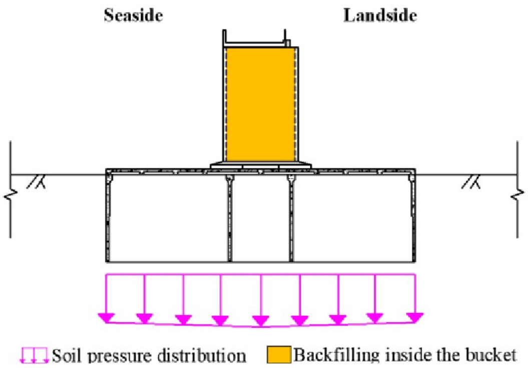

Figure 9. Simplified diagram of soil pressure distribution at the bottom of the bucket during backfilling inside the bucket.

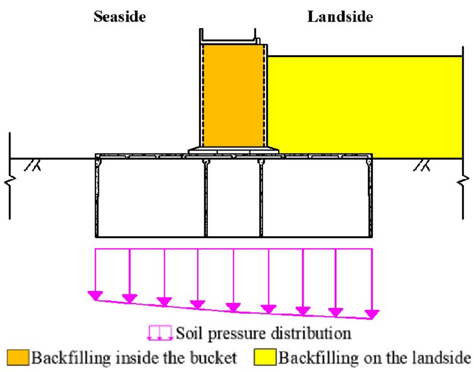

Figure 10. Simplified diagram of soil pressure distribution at the bottom of the bucket during backfilling on the landside.

To further analyse the vertical stress sharing between the bucket and soil under backfill load, the bucket-soil stress ratio (R_{bs}) was calculated. $R_{bs}=\sigma_{t9}/\sigma_{t10}$, σ_{t9} and σ_{t9} are the soil pressure measured by sensors at t9 on the cover plate and t10 on the mud surface behind the bucket, respectively. And the corresponding variation curve is shown in Figure 11. The results show that R_{bs} was close to 1 during stages I and II, suggesting a stable static water level pressure. During Stages III and IV, R_{bs} steadily increased and gradually approached a stable value. The final R_{bs} for M1 was approximately 1.50, while for M2, it was 2.06. These results imply that a larger upper backfill load results in a greater vertical load component borne by the bucket.

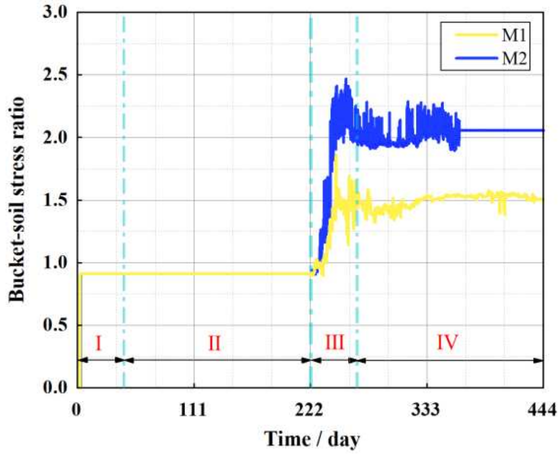

Figure 11. The variation curve of the vertical load sharing ratio between bucket and soil.

4 CONCLUSIONS

Through centrifuge model tests, the main conclusions of this study are as follows.

(1) Under varying backfill loads, the bucket exhibits different displacement modes: the primary displacement mode during backfilling inside the bucket is settlement; when backfilling with viscous materials of high water content, such as soft caly, on the landside, the dominant displacement mode is sliding towards the seaside; and when backfilling with non-cohesive materials, such as standard sand and block stones, on the landside, the primary displacement mode is overturning towards the landside.

(2) The stability during backfilling inside the bucket primarily depends on the resistance at the bucket base and the friction along the inner wall. The internal soil is mainly in a passive earth pressure state, while the external soil is close to the at-rest earth pressure state. The base resistance shows a parabolic distribution.

(3) The stability of the bucket during landside backfilling is governed by the vertical load sharing between the bucket and the surrounding soil. With increasing backfill load, the vertical load carried by the landside cover plate increases, and the bucket tends to overturn under the combined moment of the upper bucket wall and landside loading. The soil on the seaside is mainly in a passive earth pressure state, while the landside soil shows a tendency towards active earth pressure with depth. The base resistance presents a trapezoidal distribution.

ACKNOWLEDGEMENTS

The project presented in this paper is supported by the National Natural Science Foundation of China [grant numbers 52271286]; the National Key Research and Development Program of China [grant numbers 2023YFB2604200].

REFERENCES

Chen, H.F., Li, W. (2016). Centrifugal model test of bucket-based breakwater. *Port&Waterway Engineering,* 2016(03), 57-61(in Chinese). https://doi.org/ 10.16233/ j.cnki.issn1002-4972.2016.03.011

Guan Y, Pan Z, Han X. (2025). Study on the stability of bucket foundation revetment under different backfill materials: Based on geotechnical centrifugal model test. *Ocean Engineering*, 2025, 330: 121136. https://doi.org/10.1016/j.oceaneng.2025.121136

Nie, Q., Wei, B., Li, W. (2016). Centrifugal model test of bucket-based revetment stability on soft soil foundation. *Harbour Engineering,* 36(01), 37-41(in Chinese). https://doi.org/ 10.7640/zggwjs201601009

Pan, Z.J., Guan, Y.F., Han, X. (2023). Reliability analysis of bucket foundation breakwater considering water-level variations under complex natural conditions. *Engineering Failure Analysis*, 149(2023), 207250. https://doi.org/10.1016/j.engfailanal.2023.107250

Shen, X.S., Cai, Z.Y., Guan Y.F. (2017). *Research on key technologies of new bucket foundation structure*. first ed. Science Press, China(in Chinese).

Shen, X.S., Ma, Z.C. (2019). Restriction criteria for displacement of bucket-based shore-connecting structure in Xuwei Port Area. *Harbour Engineering*, 39(S1), 77-80(in Chinese). https://doi.org/10.7640/ zggwjs2019S1015

Xu, G.M., Gu, X.W., Ren, G.F. (2014). Penetration resistance and wall friction of ellipse lower bucket of breakwater into soft ground in centrifuge. *The Ocean Engineering*, 32(01), 1-7+16 (in Chinese). https:// doi.org/10.16483/j.issn.1005-9865.2014.01.011

Zhang X.Y., Gui J.S. (2018). Study on stability of bucket foundation under backfill. *IOP Conference Series: Earth and Environmental Science*, 189(4), 042019. https://doi.org/10.1088/1755-1315/189/4/042019